



Deposited via The University of Leeds.

White Rose Research Online URL for this paper:

<https://eprints.whiterose.ac.uk/id/eprint/235356/>

Version: Accepted Version

Article:

Fan, Y., Liu, A., Xie, Q. et al. (2025) Computer Vision-Driven Digitalization of the Nine Hole Peg Test Assessment Method: A Pilot Study. *Journal of Medical and Biological Engineering*, 45 (5). pp. 720-737. ISSN: 1609-0985

<https://doi.org/10.1007/s40846-025-00980-1>

Reuse

This article is distributed under the terms of the Creative Commons Attribution (CC BY) licence. This licence allows you to distribute, remix, tweak, and build upon the work, even commercially, as long as you credit the authors for the original work. More information and the full terms of the licence here:

<https://creativecommons.org/licenses/>

Takedown

If you consider content in White Rose Research Online to be in breach of UK law, please notify us by emailing eprints@whiterose.ac.uk including the URL of the record and the reason for the withdrawal request.

Computer Vision-Driven Digitalization of the Nine Hole Peg Test Assessment Method: A Pilot Study

Yuxin Fan^a, Aiqin Liu^b, Qiurong Xie^c, Qi Zhang^c, Jianyu Zhao^d, Sheng Quan Xie^e, Bo Sheng^{a,f,*}

^a School of Mechatronic Engineering and Automation, Shanghai University,
Shanghai 200444, China

^b Faculty of Biological Sciences, University of Leeds,
Leeds LS2 9JT, United Kingdom

^c College of Rehabilitation Medicine, Fujian University of Traditional Chinese Medicine,
Fujian 350122, China

^d Shanghai Rural Commercial Bank,
Shanghai 200002, China

^e School of Electronic and Electrical Engineering, University of Leeds,
Leeds LS2 9JT, United Kingdom

^f Laboratory of Intelligent Manufacturing and Robotics, Shanghai University,
Shanghai 200444, China

* Corresponding author at: School of Mechatronic Engineering and Automation, Shanghai University, 200444, Shanghai, China. E-mail address: shengbo@shu.edu.cn

Acknowledgments

The authors would like to thank Rylea Hart for the English improvement. This work was supported by the International Exchanges 2023 Cost Share (NSFC-Royal Society) under Grants [IES\R3\233204](#), the National Natural Science Foundation of China under Grants [62103252](#) and [82305357](#), and the Shanghai Magnolia Talent Plan Pujiang Project under Grants [24PJA032](#).

Abstract

Purpose: This study aimed to develop and validate a computer vision-driven Digitalized Nine Hole Peg Test (D-NHPT) to assess hand function in stroke patients, examining the reliability and validity of extracted hand features and their ability to distinguish stroke patients from healthy subjects.

Methods: A customized data collection system and an improved test device using LMC2 captured hand-motion data. The study recruited 10 stroke patients and 5 healthy subjects. Statistical analyses included intraclass correlation coefficients (ICC) for reliability, p-values for discriminant validity (Mann-Whitney U test), and |r-scores| for convergent validity.

Results: The D-NHPT demonstrated high reliability (patient group ICC=0.818–0.946; healthy group ICC=0.785–0.904), significant discriminant validity ($p < 0.019$), and strong convergent validity (|r-score|=0.671–0.909). Key features included motion speed, coordination, and task completion metrics, which effectively distinguished stroke patients from healthy subjects.

Conclusions: The D-NHPT provides a reliable, valid, and multidimensional assessment of hand function in stroke patients. Specific hand features are sensitive metrics for clinical evaluation, advancing digitalization of rehabilitation scales, and supporting personalized rehabilitation strategies.

Keywords: Stroke; Hand Function Assessment; Nine Hole Peg Test; Digitalized Assessment Scale

1. Introduction

Stroke, also known as Cerebrovascular Accident (CVA), is a cerebrovascular disorder that leads to sudden loss of brain function. Approximately 85% of stroke patients worldwide suffer from hand function impairment [1]. This impairment significantly restricts patients' ability to perform basic Activities of Daily Living (ADLs), such as tying shoelaces, wringing out a towel, and picking up and manipulating objects, which severely affects their quality of life [2]. Therefore, the hand functional evaluation for stroke patients with hand function impairment is of great importance. It is beneficial for formulating personalized rehabilitation treatment plans for patients and monitoring their rehabilitation progress. Currently, there are numerous tools for hand functional evaluation, such as the Nine Hole Peg Test (NHPT) [3], the Box and Block Test (BBT) [4], the Purdue Pegboard Test (PPT) [5], etc. These methods each have their characteristics and focuses, and they can evaluate hand function from different perspectives.

In clinical practice, the NHPT is one of the most commonly used tools for assessing hand function and has demonstrated good reliability and validity in both healthy individuals and stroke patients [3]. Compared to other assessment tools, the NHPT offers advantages such as a simple structure, low cost, and ease of transportation and management. Additionally, the test tasks are straightforward and easy to understand, making it suitable for people of all age groups. However, the NHPT has a single evaluation metric—total time to complete the test task—and does not analyze hand movement performance. This limitation makes it less conducive for therapists to develop more detailed rehabilitation treatment plans [6].

Breakthroughs in deep learning technologies have significantly enhanced the ability to conduct refined analysis of hand movements. The Temporal-Spatial Domain Adaptation (TSDA) algorithm proposed by scholars such as Shan Chunlei [7] has notably improved the accuracy of decoding movement intentions for four types of tasks (e.g., grasping, stretching) involving the unilateral upper limb in stroke patients through transfer learning between models of healthy subjects and patient data, with an average improvement of 10.3%. In addition, advancements in flexible sensors and hybrid sensing systems have provided new methods for quantifying hand function. The portable flexible rehabilitation gloves developed by the University of Science and Technology of China in 2023 [8] integrate shape memory alloy (SMA) actuators and Hall sensors, enabling real-time monitoring of finger joint angles (with an accuracy of $\pm 2^\circ$) and providing closed-loop feedback training. Clinical trials show that after 3 months of NHPT training assisted by these gloves, the average improvement in patients' independent finger movement ability (as measured by FIM scores) reached 18%.

Building on precise monitoring, the rise of lightweight assessment systems has promoted the popularization of home-based rehabilitation. The Kinect-based home aerobic exercise assessment system developed by scholars such as Huang [9] integrates the VideoPose3D human pose estimation algorithm and a heart rate monitor. It can track users' skeletal movements in real time, compare them with coaches' movements, and provide closed-loop feedback training. Clinical trials indicate that after assisting pre-frail elderly individuals in the community with 24 sessions of home-based aerobic exercise, the system significantly improved their perception of movement accuracy ($p < 0.009$) and enhanced their exercise motivation ($p < 0.001$). Moreover, their performance in moderate-intensity exercises was significantly better than that of the group without skeletal feedback. Existing technologies have reached a high level in single dimensions (e.g., AI classification accuracy, sensor precision). However, they still have limitations in terms of the stability of markerless tracking, integration with clinical tasks, and the clinical relevance of features. By integrating high-precision visual tracking, task-driven feature extraction, and multimodal data analysis, D-NHPT offers more clinically translatable solutions for the comprehensive assessment of hand function in stroke patients.

The digitalization of clinical assessment scales is currently a research hotspot. In terms of improving the traditional Nine Hole Peg Test (NHPT), one study developed the Standardized Nine Hole Peg Test (S-NHPT) and used a marker-based motion capture system to record upper limb and trunk movements during the test, proving its sufficient reliability [6]. Building on this, researchers expanded the application of sensor technology by using the Microsoft Azure Kinect to record three-dimensional coordinates of anatomical landmarks in the upper limbs and other body parts. This allowed the calculation of joint angles and spatiotemporal parameters, making the pegboard grasping task a potential standard tool for upper limb function assessment in stroke patients [10]. In the field of digital reconstruction of clinical scales, researchers proposed a new digital evaluation system to digitally reconstruct the motor function of the Wolf Motor Function Test-Functional Ability Scores (WMFT-FAS), achieving an average accuracy of 91.7% [11]. Meanwhile, for fine motor function assessment, researchers used the Leap Motion Controller (LMC) to identify sensitive kinematic features of hand movements. They analyzed 38 selected kinematic features to determine the most sensitive ones for distinguishing healthy subjects from stroke patients [12]. However, the digitalization of clinical assessment scales still requires further improvement: 1) Marker-based motion capture systems have limitations in operational efficiency and practicality (e.g., the time-consuming process of attaching markers); 2) The integration of markerless motion capture technology with NHPT remains immature.

To address the single evaluation metric of the NHPT and explore additional hand-related features for quantification, this study proposes a computer vision-based Digitalized Nine Hole Peg Test (D-NHPT) for comprehensive hand function assessment in stroke patients. Specifically, a numbered, evenly holed board replaces the original peg-container, requiring participants to insert pegs into holes in sequence for better data consistency and analysis accuracy. Also, an LMC2-based hand-motion data collection system is proposed, enabling efficient 3D hand-motion data capture. Based on this, various hand features, such as *SAL* and *Dimensionless Jerk*, are extracted for multidimensional hand-function assessment. Finally, 10 stroke patients and 5 healthy subjects are recruited for clinical testing to verify the extracted features' within-group reliability, discriminant validity, and convergent validity.

The main contributions of this study are as follows:

- 1) We enhanced and digitized the traditional NHPT into the D-NHPT, which includes an LMC2, a customized hand-motion data collection system, and a modified NHPT device, thereby enhancing the test's reliability and rigor.
- 2) We created a hand feature dataset based on the D-NHPT for constructing digital clinical assessment scales. We identified highly reliable and valid hand-sensitive metrics (ICC=0.818–0.946 for the patient group, ICC=0.785–0.904 for the healthy group, discriminant validity $p < 0.019$, $|r\text{-score}| = 0.671\text{--}0.909$), enabling more detailed hand-function assessments for stroke patients.

2. Methods

2.1 Workflow

The workflow of this study is shown in [Fig. 1](#). First, hand-motion data during the D-NHPT task is collected via the Leap Motion Controller 2 (LMC2). Then, the raw data is preprocessed, including interpolation and filtering. After preprocessing, 13 hand features (covering time and kinematic features, see [Table 1](#)) are extracted.

To validate the reliability and validity of these metrics, this study uses:

- 1) Intraclass Correlation Coefficient (ICC) for reliability analysis within the group;
- 2) Discriminant validity analysis to find feature differences between stroke patients and healthy subjects, testing the metrics' ability to distinguish groups;
- 3) Convergent validity analysis using Pearson's correlation coefficients (r) to explore the relationship between the metrics and total test time.

Finally, sensitive metrics are selected through statistical analysis to build a hand feature dataset based on the D-NHPT. This provides a scientific basis for quantitatively assessing hand function in stroke patients.

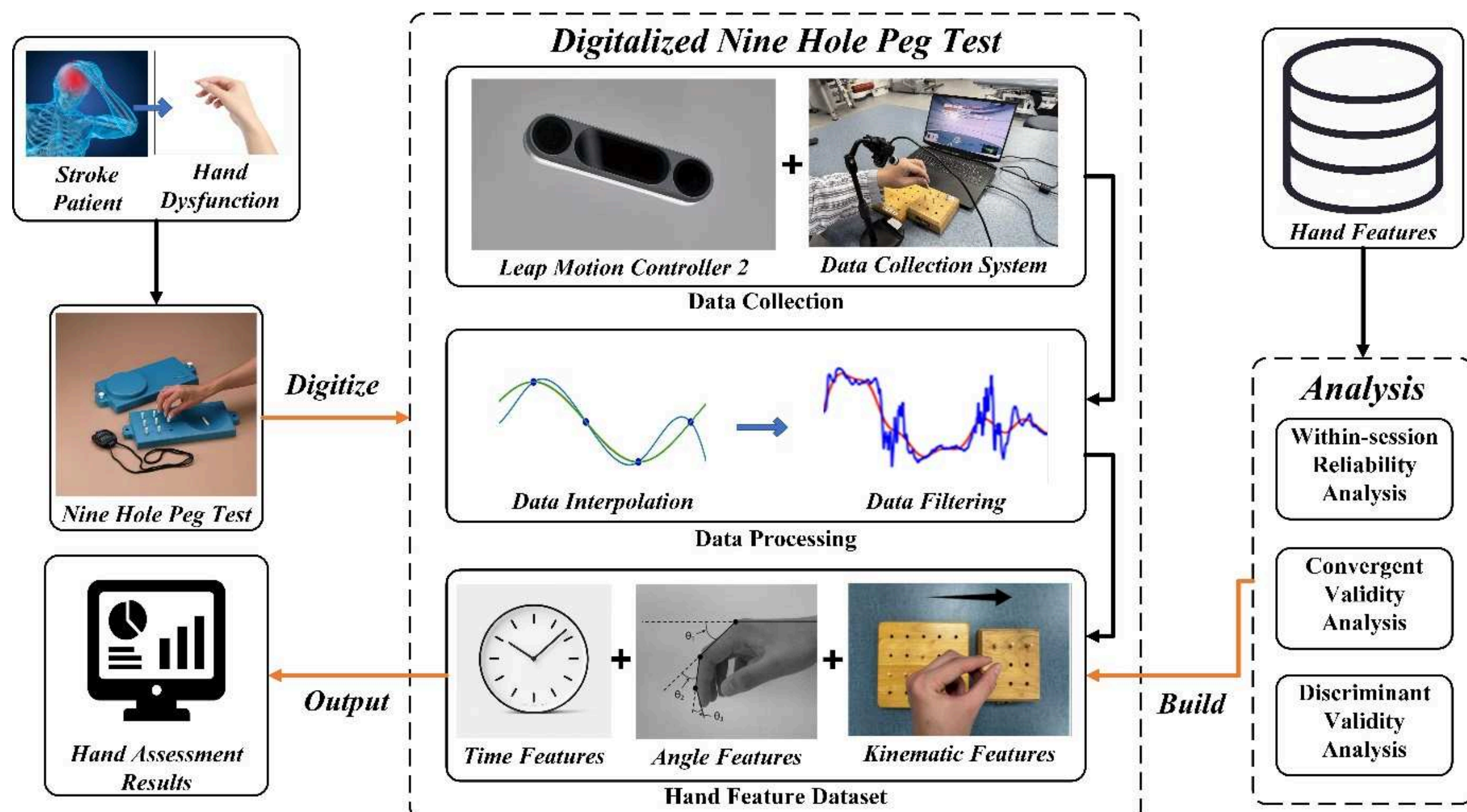


Fig. 1. The workflow of the Digitalized Nine Hole Peg Test

2.2 D-NHPT Tasks

The commonly used NHPT device includes a container, a wooden box with nine evenly distributed holes, and nine wooden pegs, as shown in Fig. 2(a). The subject is required to grasp the small wooden pegs from the container and insert them into the holes one by one, and then put these pegs back into the container one by one. This test requires the subject to complete the operation with one hand as quickly as possible. The shorter the completion time, the higher the finger flexibility of the subject. This test not only evaluates the flexibility and coordination of the hand but also reflects fine motor skills, and it is a relatively comprehensive hand function test [13].



(a) The commonly used NHPT Device

(b) The D-NHPT Device

Fig. 2. Comparison Diagram of NHPT Devices

In the D-NHPT, a complete process requires the patient to insert the pegs into the holes one by one as quickly as possible. The time period from when the patient touches the first peg to when the last peg is completely put down is recorded as the total completion time. In order to conduct a more meticulous and precise analysis of the patient's motor performance, this study used a wooden board with evenly distributed holes to replace the original peg placement container of the NHPT device. As shown in Fig. 2(b), the holes were numbered, and it was specified that the subjects should insert the pegs into the corresponding holes according to the numbers. Then, according to the research of scholars such as Johansson [6] and Temporiti [14], the entire movement process was divided into four movement stages: The picking-up Stage, Moving Stage, Placing Stage, and Returning Stage. Fig. 3 is a schematic diagram of the movement decomposition of the D-NHPT. The definitions of each stage and the transition criteria are shown in Table 1.

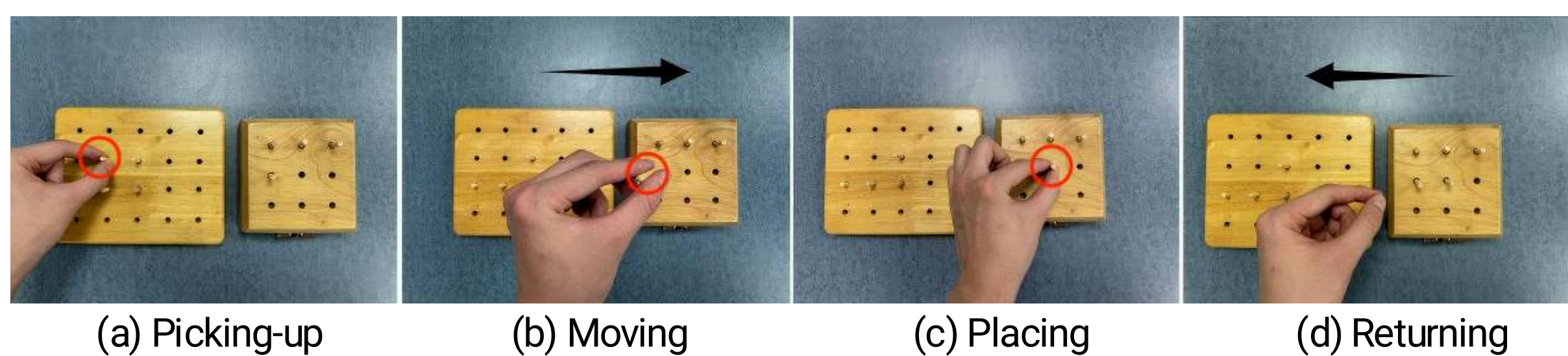


Fig. 3. Schematic Diagram of D-NHPT Action Decomposition

2.3 Application development

In terms of data collection, the latest LMC2 from Ultraleap is used as the collection device. For hand-data collection, marker-based motion-capture systems have limitations such as high costs and marker occlusion. Moreover, attaching markers to participants' hands is time-consuming. Therefore, using a markerless motion-capture system facilitates hand-data collection. Compared with the previous LMC and Stereo IR 170, the improvements of the LMC2 make the hand-tracking technology more ideal. Several studies have shown [15, 16] that the LMC2 can reliably and accurately capture hand-motion data and objectively assess hand function. At the start of the test task, participants place the hand to be tested (the affected hand for stroke patients and the dominant hand for healthy subjects) on the table, with the upper arm in a neutral position and the elbow bent at about 90 degrees (as shown in Fig. 4(a)). In addition, this study has developed a non-contact hand-motion data collection system for data collection and storage. The system provides three collection modes: "Track Left Hand", "Track Right Hand", and "Track Both Hands". The system not only realizes markerless collection and real-time monitoring of the collection status but also ensures the

accuracy of data collection and the reliability of storage. The overall interface is shown in Fig. 4(b).



(a) Schematic of Hand Placement System

(b) Interface of Hand-Motion Data Collection System

Fig. 4. Schematic of Hand Placement and Interface of Hand-Motion Data Collection System

The setup time for D-NHPT is approximately 2 minutes, including connecting the LMC2 to the computer via a data cable, launching the hand movement data acquisition system on the computer, and setting relevant parameters within the system. In addition, the LMC2 relies on an infrared camera to track hand movements; strong light, backlight, or environments with low light contrast may reduce tracking accuracy, while regular indoor or outdoor lighting conditions are sufficient for operation. Meanwhile, occlusion of the hand may interfere with tracking, so it is necessary to ensure that the acquisition scene is simple and free of obstructions.

2.4 Data processing

In this study, the LMC2 was used for data collection. Due to the large movement amplitude of the D-NHPT, there are significant differences between consecutive data points. To ensure the integrity and continuity of the dataset, this study first employed the cubic spline interpolation method to resample the collected data. Cubic spline interpolation is a widely used technique in spline function interpolation problems, favored for its excellent approximation capability and smoothness [17]. The formula for cubic spline interpolation is shown as follows:

$$S(x) = a_i + b_i(x - x_i) + c_i(x - x_i)^2 + d_i(x - x_i)^3 \quad \#(1)$$

In the actual data collection process, it may be interfered with by various objective factors such as noise signals and changes in lighting conditions. These factors may all lead to data jitter or anomalies. In order to ensure the accuracy and reliability of data analysis, before conducting data analysis, it is necessary to smooth the key point data of the hand. The Singular Spectrum Analysis (SSA) algorithm [18] is an efficient time

series analysis method, which is particularly suitable for smoothing the original motion data. Compared with traditional filtering methods, the SSA algorithm has shown good effects in removing noise and improving data quality [19]. Therefore, this study uses the SSA algorithm to filter the collected data to improve the accuracy and reliability of subsequent analyses. The representation of the matrix is shown as follows:

$$X_L = (x_{ij})_{i,j=1}^{L,K} = \begin{pmatrix} x_1 & x_2 & x_3 & \cdots & x_K \\ x_2 & x_3 & x_4 & \cdots & x_{K+1} \\ \vdots & \vdots & \vdots & \ddots & \vdots \\ x_L & x_{L+1} & x_{L+2} & \cdots & x_N \end{pmatrix} \#(2)$$

The performance of the SSA algorithm mainly depends on two parameters: the window length L and the number of maximum eigenvalues [20]. In this study, the window length is set to 99, and the number of maximum eigenvalues is set to 3 [21, 22]. Experimental verification was carried out according to these settings, and the results show that the SSA algorithm can effectively smooth the three-dimensional data and, at the same time, better retain the authenticity of the original data during the smoothing process. The SSA algorithm filtered the motion trajectory collected by the hand motion system. The images before and after the filtering process are shown in Fig. 5, which displays the curve of the three-dimensional coordinates of the index finger tip changing with the time series.

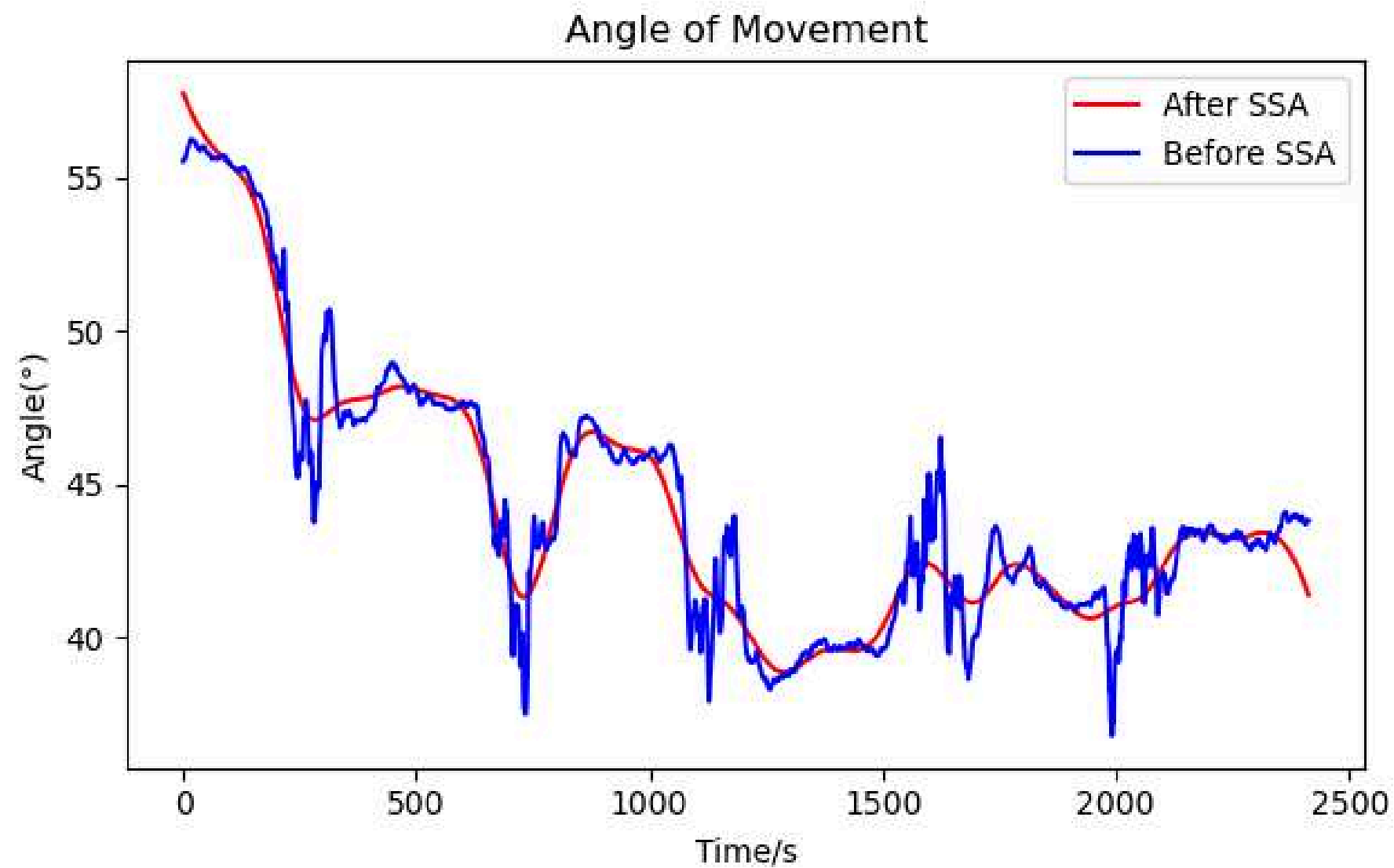


Fig. 5. Comparison of Data Before and After Filtering Using the SSA Algorithm

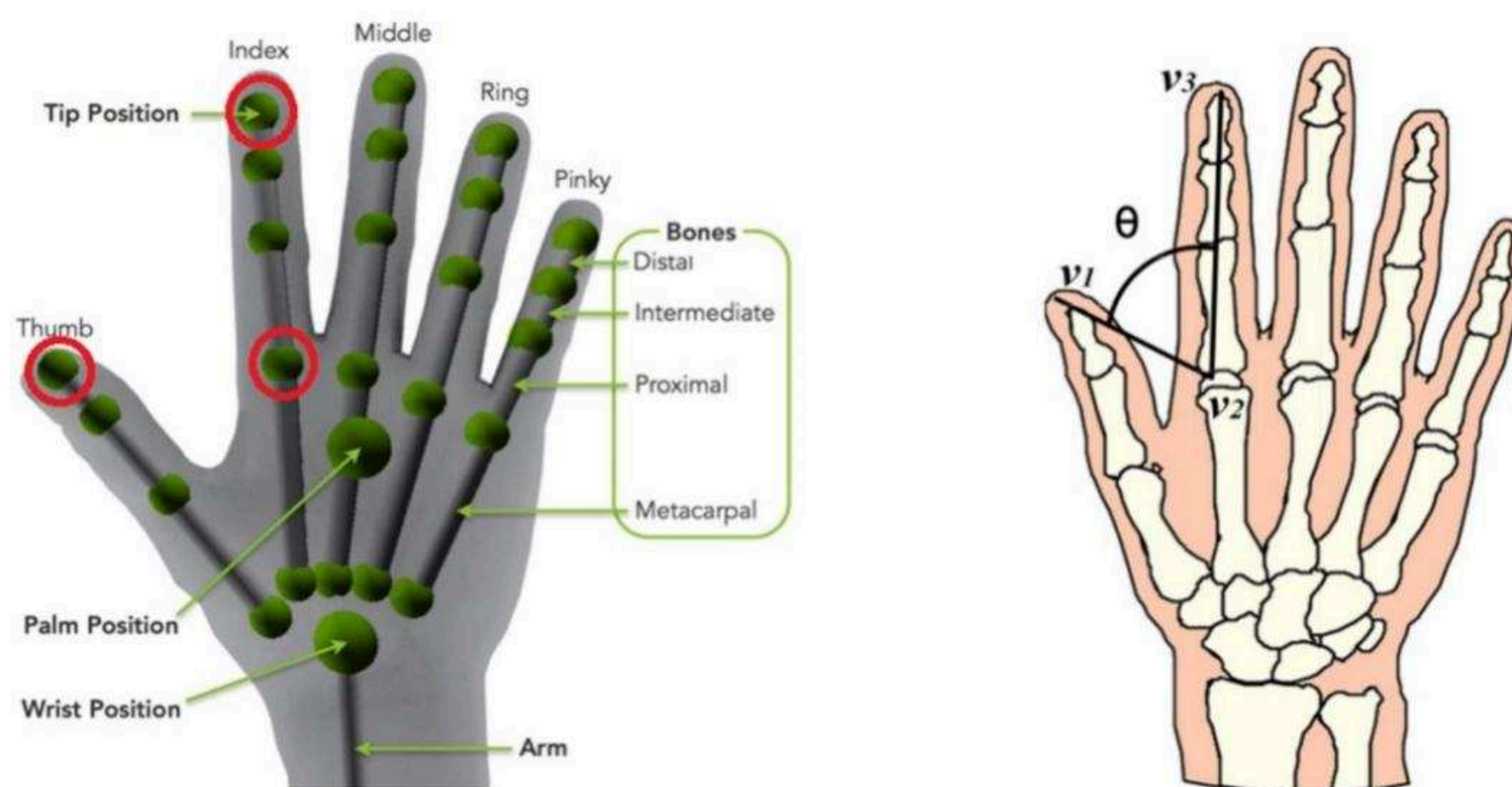
2.5 Data processing

In order to transform the collected raw data into information with evaluation value, this study mainly extracted 13 characteristics and divided them into three main aspects (Table 2):

- 1) Time features (5 items, *Total time*, *Time for the Picking-up/Moving/Placing/Returning stage*, *Grasp-Reach Ratio*);
- 2) Kinematic features (8 items, such as *Dimensionless Jerk*, *Index Finger Path Ratio*).

2.5.1 Angle Range

Due to individual differences in hand size and relative position, hand joint vectors vary and cannot directly serve as motion assessment features. Studies show that during the same motion, hand-motion patterns and trends in inter-joint angle changes are generally consistent, but the sensitivity to angle changes varies across different joints [23]. Therefore, this study selected three key points based on the 26 hand skeletal points captured by the LMC2 and doctors' advice: the thumb tip to index finger metacarpophalangeal (MCP) joint and the index fingertip to index finger MCP joint (Fig. 6(a)). The angles between these points (opening/closing angles) were used as key parameters for analysis (Fig. 6(b)).



(a) The hand-skeleton key points captured by the LMC2 and the schematic of the selected key points (b) Diagram of Angular Configuration

Fig. 6. Diagram of Angle Range

2.5.2 Time and Kinematic Features

- 1) Time and Velocity Features

In the D-NHPT, the *Total Time* (T) required to complete the entire movement was calculated, as well as the time required for each movement stage: namely, the *Time of the Picking-up Stage* (t_1), the *Time of the Moving Stage* (t_2), the *Time of the Placing Stage*

(t_3), and the *Time of the Returning Stage* (t_4). Also, the *Peak Velocity at the Moving Stage* (V_{1max}), the *Peak Velocity at the Returning Stage* (V_{2max}), and the *Average Velocity* (V_{mean}) were measured.

2) *Grasp-Reach Ratio (GRR)*

Stroke patients often exhibit significantly increased time consumption in the manipulation phase (the Picking-up Stage and the Placing Stage), such as unstable grasping and difficulty in peg insertion. In contrast, the transfer phase (the Moving Stage and the Returning Stage) is relatively preserved (pertaining to upper arm movements). To quantify the time allocation between the two phases through a ratio, which can reveal subtle motor deficits that cannot be captured by traditional total time, this study introduces the ratio of the time consumed in the manipulation phase to that in the transfer phase, referred to as the *Grasp-Reach Ratio (GRR)* [6]. The calculation formula for this ratio is as follows:

$$GRR = \frac{t_1 + t_3}{t_2 + t_4} \quad \#(3)$$

3) *Index Finger Path Ratio (Path)*

In order to accurately evaluate the movement efficiency of the subjects during the D-NHPT tasks, this study introduces the *Index Finger Path Ratio (Path)*, which is the ratio of the actual movement path length of the subject's index finger to the length of the straight-line path under ideal conditions. This ratio is helpful for analyzing the hand coordination and the efficiency of movement control of the subjects. Similarly, by calculating the maximum speed and the average speed of the tip of the index finger during the movement process, the hand flexibility and fine motor coordination ability of the subjects can be further evaluated, thus enhancing the reliability of the research results. The calculation formulas are as follows:

$$Path = \frac{S_a}{S_i} \quad \#(4)$$

Among them, S_a represents the actual movement path of the index finger, and S_i represents the ideal movement path. The closer the *Path* value is to 1, the higher the movement efficiency of the subject is, and the higher the accuracy of the hand movement is. On the contrary, the larger the *Path* value is, the more the subject's movement path deviates from the ideal state, and the lower the movement efficiency is.

4) *Spectrum Arc Length (SAL)* and *Dimensionless Jerk (J*)*

Stroke often affects the patient's ability to control the neural system, leading to pauses, tremors, or unexpected movements during the movement process. In this context, the smoothness of movement reflects the continuity, coordination, and control ability of movement execution [24]. Quantitative analysis of the smoothness of movement is helpful for evaluating the effectiveness of rehabilitation training, providing a scientific basis for formulating personalized rehabilitation programs, and thus more effectively promoting the recovery of hand function and improving the operational ability in daily life [25].

Firstly, the smoothness of movement can be evaluated by calculating the *Spectrum Arc Length (SAL)* of the velocity profile [26]. This method holds that the continuity and smoothness of movement are usually related to the frequency components. Unsmooth movements (such as sudden stops or accelerations) will introduce higher-frequency components. Scholars such as Sheng [27] adopted *SAL* as a feature for evaluating motor smoothness. They quantified motor smoothness by calculating *SAL* values of movements, including endpoints and shoulder flexion, adduction, and internal rotation.

When using the *SAL* to evaluate the smoothness of movement, it is first necessary to perform a Fourier transform on the signal to obtain the frequency-domain representation. Then, calculate the *SAL*:

$$X(f) = F\{x(t)\} \quad (5)$$

$$SAL = \int_{f_1}^{f_2} \sqrt{1 + \left(\frac{d|X(f)|}{df} \right)^2} df \quad (6)$$

where F represents the Fourier transform, $x(t)$ is the time-domain signal, $X(f)$ is the corresponding frequency-domain signal, and f represents the frequency, f_1 and f_2 define the frequency range of the analyzed signal, and $|X(f)|$ represents the amplitude spectrum of the signal $X(f)$ in the frequency-domain representation. *SAL* represents the length of the curve on the spectrum from point f_1 to point f_2 . If the signal changes gently, its derivative is small, meaning that the *SAL* value is small. Conversely, if the signal changes drastically, the derivative increases, and the corresponding *SAL* value is also large. By analyzing the *SAL* value, it is possible to evaluate the smoothness of the signal quantitatively and further determine its dynamic characteristics.

In addition, *Dimensionless Jerk (J^*)* assesses motor smoothness by utilizing dimensionless changes in acceleration. In the field of kinematics, Jerk is regarded as a key indicator for evaluating motor smoothness [28]. Specifically, the smaller the change in acceleration during movement, the smoother the movement tends to be. Scholars such as Temporiti [14] found that Normalized Jerk can sensitively reflect

differences in hand movement smoothness with good reliability and validity. Specifically, *Dimensionless Jerk* assesses motor smoothness by calculating the second time derivative of acceleration, followed by time integration and dimensionless processing of the results. The specific solution formula is as follows:

$$\begin{cases} J = \frac{d^2v}{dt^2} \\ J^* = \frac{\int |J(t)| dt}{a_{max} \cdot T^2} \end{cases} \quad \#(7)$$

where J represents the Jerk, a_{max} represents the maximum acceleration, and T is the time interval. The smaller the value of J^* , the smaller the rate of change of acceleration during the motion process, which means the motion is smoother. The larger the value of J^* , the higher the rate of abrupt change of acceleration during the motion process, reflecting more drastic motion changes.

3. Experiments

3.1 Participants

As the preliminary clinical validation of the D-NHPT, this study aims to preliminarily examine the feasibility of the method, the stability of data collection, and the sensitivity of core indicators. This study recruited 10 stroke patients (9 males and 1 female, aged 57 ± 12.51 years). The inclusion criteria for stroke patients are as follows: 1) Patients with stroke meeting international stroke diagnostic criteria and confirmed by cranial CT or MRI; 2) The patient is in the subacute phase of stroke (more than 7 days to 6 months); 3) Brunnstrom stages V-VI; 4) Stable medical condition with sufficient endurance to complete the study; 5) Normal cognitive function, ability to understand study instructions, and willingness to provide written informed consent. These patients were all able to perform relatively complex hand movements but still had coordination and control disorders. Meanwhile, 5 healthy subjects were also recruited as a control group, including 3 males and 2 females, with an average age of 24 years. The specific information of the subjects is shown in [Table 3](#). All subjects had no neurological or musculoskeletal system diseases or cognitive impairments and were able to complete the specified actions independently. Before the experiment, the purpose and method of this experiment were explained in detail to the subjects, and all of them signed the informed consent form. In addition, this study has been approved by the Ethics Committee of Shanghai University (Approval No.: ECSHU 2021-102).

The Brunnstrom Scale is used to evaluate the recovery of motor function [29]. This scale is mainly divided into three parts: the upper limb, the hand, and the lower limb, and the recovery process is divided into six distinct stages (as shown in [Table 4](#)).

The Berg Balance Scale is used to evaluate the patient's ability to actively shift the body's center of gravity [30]. The scale consists of a total of 14 assessment items, covering common balance movements in daily life. The score range for each item is from 0 to 4 points, so the highest total score is 56 points. The higher the score, the stronger the patient's balance ability.

3.2 Testing protocol

The complete experimental procedure of the D-NHPT tasks is as follows: The subject sits on a stool with a height of 40 cm and places both hands naturally on a table with a height of 90 cm. After the experimenter gives the instruction of "start", the subject lifts the affected hand, picks up only one wooden stake each time, and moves the wooden stakes one by one from the placement container to the corresponding holes in the nine-hole wooden box. The time from when the subject touches the first wooden stake until the last wooden stake is put down is recorded as one experiment. Each subject needs to conduct 3 experiments. The interval between tests should be such that the subject does not feel fatigued, usually not less than 20 seconds. The experimental diagram of the subject is shown in [Fig. 7](#).

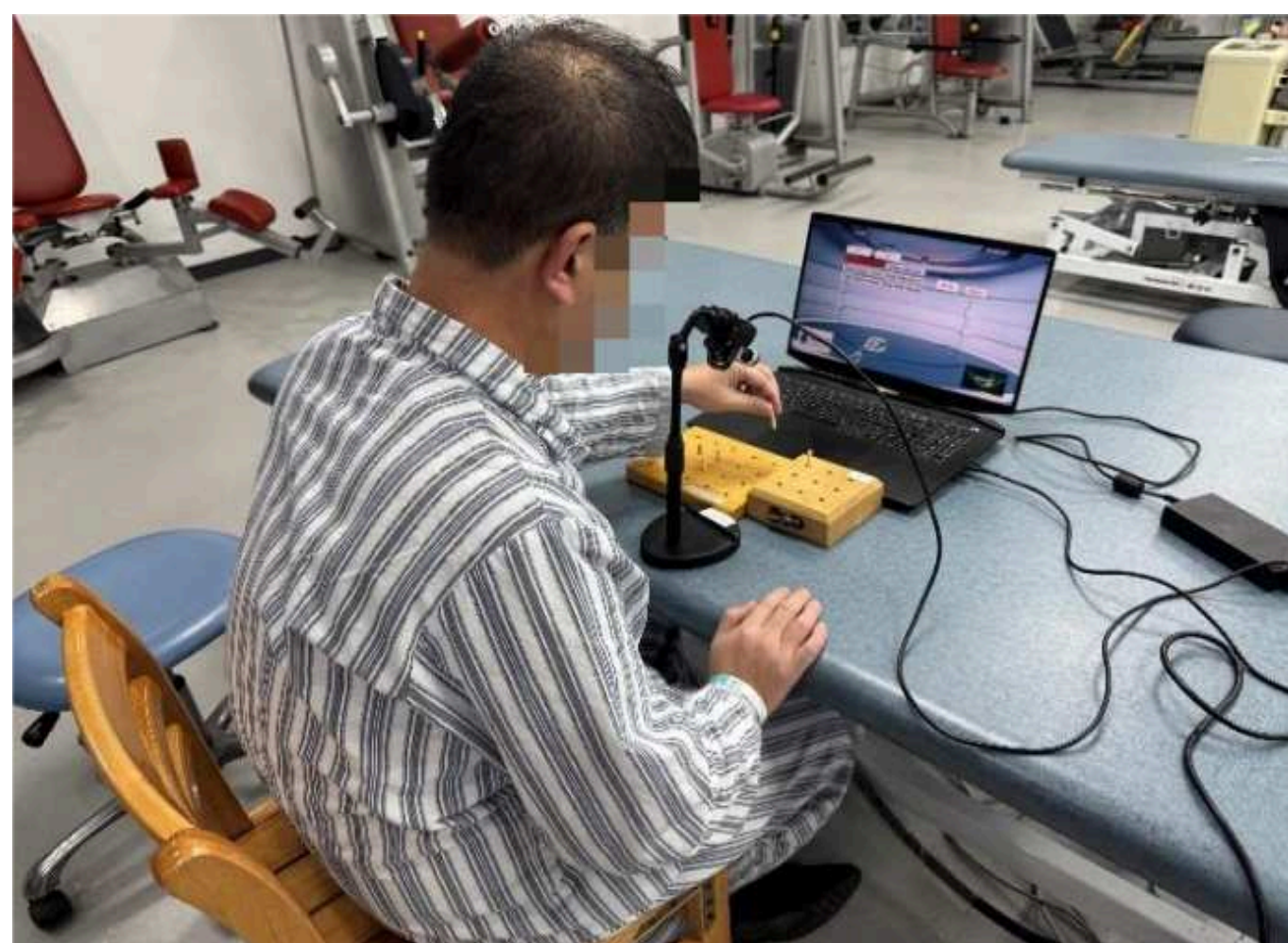


Fig. 7. Schematic Diagram of Participants Conducting the Digitalized Nine Hole Peg Test

3.3 Statistical analysis

First, in this study, Intraclass Correlation Coefficients (ICC) were used to assess the Test-Retest reliability. The Confidence Interval (CI) was set at 95%. The numerical standards for ICC are as follows: 0.00-0.50 indicates poor reliability, 0.50-0.75 indicates

moderate reliability, 0.75-0.9 indicates good reliability, and above 0.9 indicates excellent reliability [31].

In addition, this study calculated the Mean Difference (MD) and Standard Error (SE) to provide more accurate estimates of measurement error. Specifically, the MD represents the mean difference in a particular feature metric between the patient group and the healthy group, while the SE quantifies the variability of the MD. The calculation formula is as follows:

$$SE = \sqrt{\frac{s_1^2}{n_1} + \frac{s_2^2}{n_2}} \quad \#(8)$$

where s_1 and s_2 are the sample standard deviations of the feature metric for the patient group and the healthy group, respectively, and n_1 and n_2 are the sample sizes of the patient group and the healthy group, respectively.

Finally, Pearson's correlation coefficients (r) were used to explore the correlation between the hand features and the total time. According to the Pearson correlation coefficient, the strength of the relationship is classified as follows: an absolute value of the r -score below 0.3 is considered a weak correlation, an absolute value between 0.3 and 0.6 is considered a moderate correlation, and an absolute value above 0.6 is considered a strong correlation [32].

Statistical analysis was performed using IBM SPSS (Statistical Package for the Social Sciences, Version 21.0), and the selected significance level was 0.05.

4. Results

4.1 Test-Retest

This study mainly focused on the Intraclass Correlation Coefficient (ICC) of these hand features in the Test-Retest scenario. As can be seen from [Table 5](#), no significant differences were found between the Test-Retest of all features. Among stroke patients, the ICCs of t_1 , t_3 , t_4 , and SAL are between 0.904 and 0.946; the ICCs of T , t_2 , and V_{mean} are between 0.818 and 0.858; the ICCs of GRR , Angle Range, $Path$, $V_{1\text{max}}$, $V_{2\text{max}}$, and J^* are between 0.539 and 0.729; the p -values of all features are less than 0.001. Among healthy subjects, t_3 has the highest ICC value, reaching 0.904; the ICCs of GRR , $V_{1\text{max}}$, $V_{2\text{max}}$, and J^* are between 0.714 and 0.749, and the ICCs of the remaining features are between 0.795 and 0.892; similarly, the p -values of all features are less than 0.001.

4.2 Time Features

[Table 6](#) shows the time features of all subjects participating in the test task, covering various time data and the GRR . In the patient group, P5 had the longest total time,

which was 100.92 seconds, while P6 had the shortest total time, which was 20.7 seconds. In the group of healthy subjects, H4 had the shortest total time, which was 11.65 seconds, and H2 had the longest total time, which was 13.8 seconds. Overall, the stroke patients performed the Nine Hole Peg Test significantly slower than the healthy subjects. The average difference in total time was $SD=35.53$ seconds, and the standard error was $SE=7.68$ seconds. Specifically, for each action stage, in the Picking-up Stage (t_1), the time spent by the patient group was between 4.71 seconds (P7) and 22.29 seconds (P9), while that of the healthy subject group was between 1.7 seconds (H5) and 2.54 seconds (H2). In the Moving Stage (t_2), the time range of the patient group was from 3.83 seconds (P7) to 12.54 seconds (P9), and that of the healthy subject group was from 3.18 seconds (H1) to 4.14 seconds (H3). In the Placing Stage (t_3), the time of the patient group ranged from 7.81 seconds (P6) to 90.99 seconds (P5), while that of the healthy subject group was between 3.36 seconds (H5) and 4.27 seconds (H1). In the Returning Stage (t_4), the time of the patient group was between 3.22 seconds (P7) and 8.09 seconds (P9), and that of the healthy subject group was between 2.85 seconds (H4) and 3.72 seconds (H3). There were differences in the time of each stage between the two groups. The specific differences were 11.21 seconds for the Picking-up Stage, 3.66 seconds for the Moving Stage, 20.89 seconds for the Placing Stage, and 2.47 seconds for the return stage. In addition, the *GRR* also showed significant differences between the two groups. The *GRR* values of the stroke patient group fluctuated greatly, ranging from 1.49 (P6) to 6.91 (P5), with an average value of 2.83. The *GRR* values of the healthy subject group were more concentrated, ranging from 0.71 (H3) to 1.05 (H1), with an average value of 0.85.

4.3 Kinematic Features

[Table 7](#) shows the data results of kinematic features for the stroke patient group and the healthy subject group. The data shows that the *Path* of stroke patients was significantly higher than that of healthy subjects, with an average difference of $SD=0.208$ mm, a standard error of $SE=0.097$ mm, and $p<0.05$. In the patient group, P5 had the highest *Path* (1.93), and P7 had the lowest (1.00). In the healthy subject group, H5 had the highest *Path* (1.28), and H3 had the lowest (1.05). It was further found that the Angle Range of stroke patients during the operations of grasping and placing wooden stakes was significantly smaller than that of healthy subjects, and the difference was highly statistically significant ($p<0.001$). The range of the Open-Close Angle in the patient group was from 8.30° (P7) to 19.83° (P3), while that in the healthy subject group was from 29.52° (H5) to 39.83° (H1). In addition, there were no significant differences in V_{1max} and V_{2max} between stroke patients and healthy subjects. In the patient group, V_{1max} was between 0.19 (P4) and 0.93 (P3), and V_{2max} was

between 0.21 (P5) and 1.16 (P3). In the healthy subject group, the range of $V_{1\max}$ was from 0.25 (H1, H5) to 0.32 (H3), and $V_{2\max}$ was between 0.26 (H5) and 0.39 (H3). The V_{mean} of patients was significantly lower than that of healthy subjects (the average value of the patient group=0.08m/s and the average value of the healthy subject group=0.108m/s). The T-test showed that this result had a statistically significant difference ($p=0.036$). In the patient group, P9 had the lowest average velocity (0.05m/s), and P6 had the highest (0.12m/s). In the healthy subject group, H3 had the highest average velocity (0.14m/s), and H4 had the lowest (0.09m/s). The two features of SAL and J^* also showed significant differences between the two groups. The SAL values of the patient group were between -49.3 (P6) and 11.34 (P8), and those of the healthy subject group were between -8.13 (H4) and 5.1 (P7). The Dimensionless Jitter J^* values of the patient group were between -39.7 (P5) and 27.11 (P2), and those of the healthy subject group were between -27.11 (H2) and 26.29 (H4).

Fig. 8 shows a comparison of the index finger movement trajectories between stroke patients and healthy subjects. As can be seen from the figure, the movement trajectories of stroke patients exhibit more tremors, while the movements of healthy subjects are smoother. In addition, when analyzing velocity changes, this study defined the hand movement from left to right as positive velocity and from right to left as negative velocity. In the index fingertip velocity change curve (**Fig. 9**), the velocity change curve of healthy subjects is smoother. At the same time, stroke patients show more significant velocity fluctuations, especially near the zero point where the velocity transitions, and there is a brief fluctuation phenomenon.

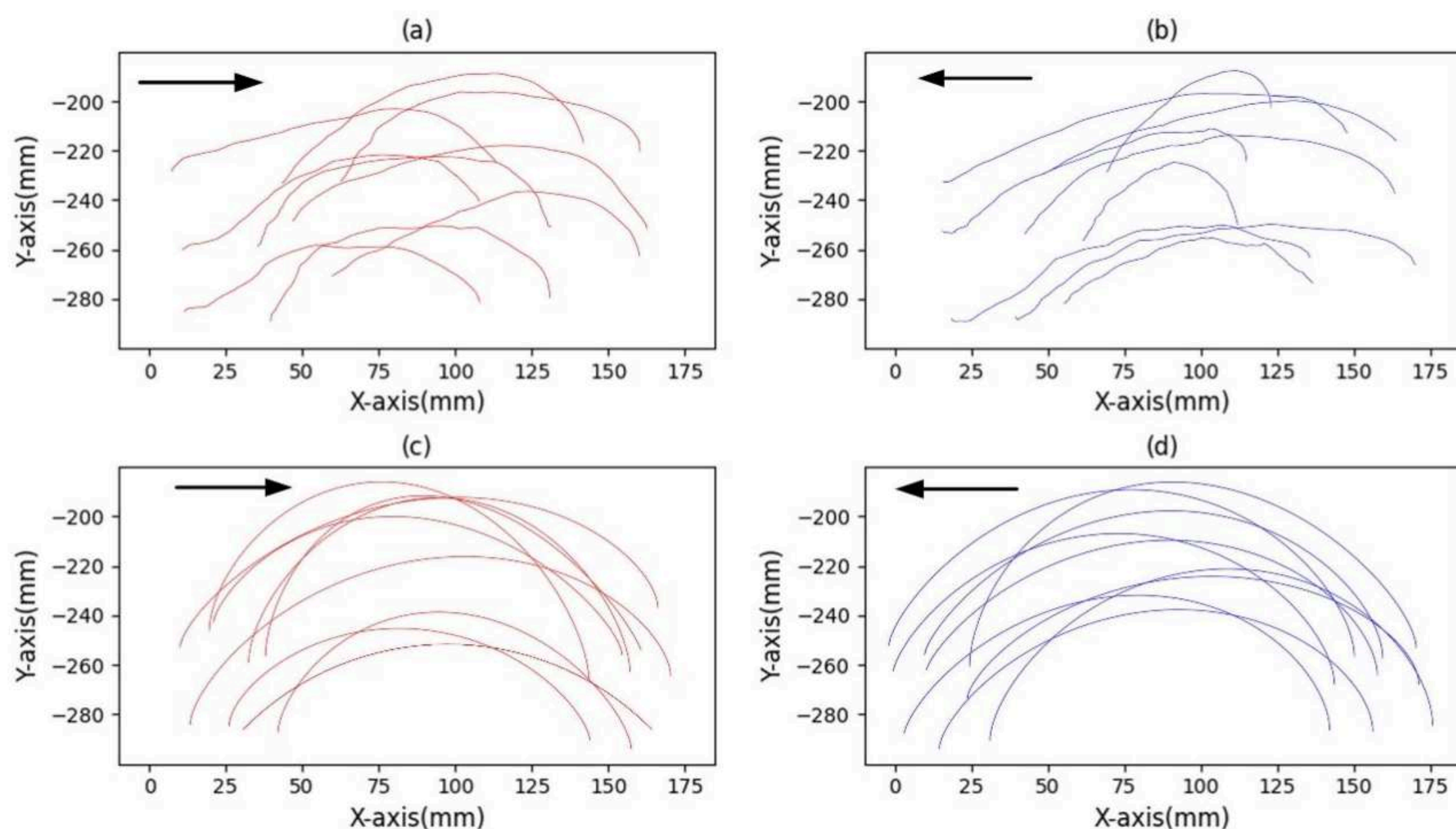
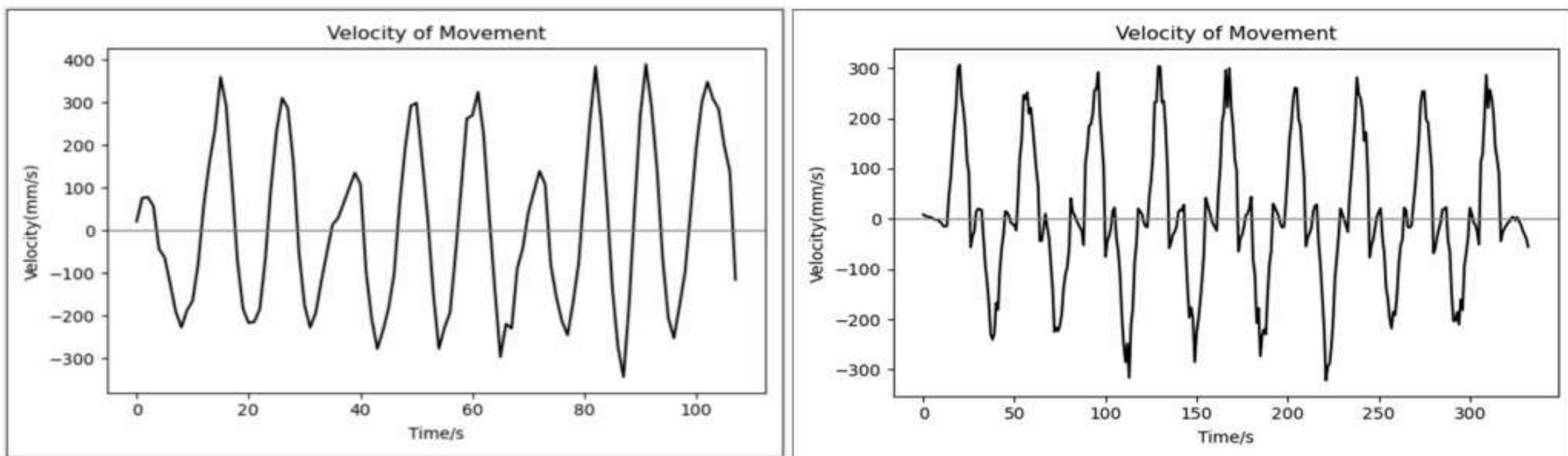


Fig. 8. Index Finger Movement Trajectories of Participants

(Figures (a) and (b) show the index finger movement trajectories of stroke patients, while figures (c) and (d) show the index finger movement trajectories of healthy subjects.)



(a) Speed Variation of Healthy Subjects

(b) Speed Variation of Stroke Patients

Fig. 9. Comparison Diagram of the Speed Variation Curves of the Participants

4.4 Convergent Validity

In the traditional evaluation scheme of NHPT, total time is an important weight for physical therapists when evaluating patients. To verify the correlation between the included features and the total time, this study used the Pearson correlation coefficient (r) for evaluation. Table 8 shows the Pearson correlation coefficients between each feature and the total time in order to quantify the strength of the association between these features and the total time. The data shows that t_1 , t_2 , t_3 , t_4 , GRR, and *Path* are all significantly positively correlated with the T . Among them, the t_3 has the strongest correlation with the total time, with an r -score reaching 0.909, $p < 0.001$; the r -score of the GRR is 0.907, $p < 0.001$; the r -score of t_4 is 0.855, $p < 0.001$; the r -score of t_1 is 0.74, $p = 0.002$; the r -score of the *Path* is 0.724, $p = 0.002$; the r -score of t_2 is 0.693, $p = 0.004$. Angle Range, V_{mean} , SAL, and J^* are negatively correlated with T . Among them, V_{mean} and J^* show a strong negative correlation. The r -score of the V_{mean} is -0.765, $p < 0.001$; the r -score of J^* is -0.833, $p < 0.001$; the r -score of the SAL of motion is -0.671, $p = 0.006$; the r -score of Angle Range is -0.543, $p < 0.001$. The correlations between $V_{1\text{max}}$, $V_{2\text{max}}$, and T are not significant. The r -score of $V_{1\text{max}}$ is 0.282, $p = 0.309$; the r -score of $V_{2\text{max}}$ is 0.135, $p = 0.631$.

5. Discussion

The main findings of this study are as follows: 1) The proposed D-NHPT can conduct a multidimensional and comprehensive assessment of hand function in stroke patients based on the hand feature dataset it constructs. 2) Hand features, such as SAL, demonstrate excellent within-group reliability (ICC=0.818–0.946 for the patient group, ICC=0.785–0.904 for the healthy group), discriminant validity ($p < 0.019$), and

convergent validity ($|r\text{-score}|=0.671-0.909$). These features can serve as sensitive metrics for assessing hand function, which is of great significance for analysing the hand movements of stroke patients and devising rehabilitation plans.

5.1 Within-group Reliability Analysis

The Within-group Reliability Analysis of hand features reflects their reliability and is quantitatively evaluated through the intra-class correlation coefficient (ICC). Further analysis of the patient's motion data shows that the time in t_1 , t_3 , t_4 , and the SAL show excellent reliability (ICC=0.904-0.946, $p<0.001$), while T , t_2 , and V_{mean} demonstrate good reliability (ICC=0.818-0.858, $p<0.001$). Meanwhile, GRR , Angle Range, $Path$, $V_{1\text{max}}$, $V_{2\text{max}}$, and J^* show moderate reliability (ICC=0.539-0.729, $p<0.001$). Among healthy subjects, t_3 has excellent reliability (ICC=0.904, $p<0.001$), and GRR , $V_{1\text{max}}$, $V_{2\text{max}}$, and J^* all exhibit moderate reliability (ICC=0.714-0.749, $p<0.001$), and the remaining features all show good reliability (ICC=0.795-0.892, $p<0.001$). Since these features cover different aspects of hand movements, such as the efficiency and speed of task execution, this makes the conclusion more comprehensive and objective. In conclusion, the hand features extracted by the hand motion data acquisition system built based on LMC2 exhibit good reliability.

5.2 Discriminant Validity Analysis

As shown in [Table 9](#), first, in terms of temporal features, stroke patients' performance in the D-NHPT is significantly slower than that of healthy subjects (the mean total time (T) for the patient group is 48.386s, while that for the healthy group is 12.86s, $p<0.001$). Specifically, the mean differences (MD) between the two groups in the stages of picking up (t_1), moving (t_2), placing (t_3), and returning (t_4) are 11.212s, 3.658s, 20.89s, and 2.465s, respectively. These differences further indicate that stroke patients have difficulties in performing fine and coordinated movements. In addition, the GRR also shows a significant difference between the two groups (the mean for the patient group is 2.83, while that for the healthy group is 0.846, $p=0.001$). This difference suggests that stroke patients spend more time in the manipulation stage relative to the transfer stage, which may be related to impaired neuromuscular control and limited motor function.

Second, in terms of kinematic features, the path ratio of the index finger of stroke patients is significantly higher than that of healthy subjects (MD=0.208 mm, SE=0.10 mm, $p=0.036$), indicating that patients travel a longer total distance with their hands in this test. Further analysis reveals that the angle range during grasping and placing pegs

for stroke patients is significantly smaller than that for healthy subjects (the mean for the patient group is 11.754° , while that for the healthy group is 35.06° , $p < 0.001$). This indicates that the opening and closing angle between the thumb and index fingertips of stroke patients is more restricted when performing such fine motor tasks. In addition, there are no significant differences between stroke patients and healthy subjects in the peak velocity features $V_{1\max}$ ($p = 0.231$) and $V_{2\max}$ ($p = 0.166$). This result indicates that, in the context of the present study, $V_{1\max}$ and $V_{2\max}$ have limited clinical value in distinguishing differences in hand function between stroke patients and the healthy population. However, findings from Johansson et al. show that the peak speed (Peak Speed) indicator can effectively differentiate motor performance between stroke patients and healthy subjects, which suggests that it still holds research significance. However, analysis of mean velocity (V_{mean}) shows that the V_{mean} of stroke patients is significantly lower than that of healthy subjects (the mean for the patient group is 0.08 m/s, while that for the healthy group is 0.108 m/s), with a statistically significant difference in the T-test ($p = 0.014$). This reflects that, due to limitations in hand-motor function, stroke patients have a slower overall movement velocity when performing the same action. Finally, significant differences are also observed between the two groups in *SAL* ($p < 0.001$) and *Dimensionless Jerk* (J^*) ($p = 0.003$), indicating that the hand-movement process of stroke patients involves more discontinuities and tremors. Compared with healthy subjects, stroke patients perform worse in fine motor control. Carpinella et al. [23] found that the peak velocity of joint movement during hand-opening and -closing actions in stroke patients was significantly lower than that in healthy subjects, which is different from the results of this study and may be due to differences in the selected test actions. Except for the peak velocity features $V_{1\max}$ and $V_{2\max}$, the other features can effectively distinguish stroke patients from healthy subjects; that is, they have good discriminant validity, which is consistent with the results of Peter et al. [13].

Fig. 8 and Fig. 9 show the comparison of the movement trajectories between stroke patients and healthy subjects. It can be seen that the movement trajectories of stroke patients have more jitters, which reflects the incoherence of their hand movements, consistent with the analysis results in Table 7. That is, the patients have a lower smoothness of movement. In addition, as shown in Fig. 9, the velocity change curve of healthy subjects is relatively smooth, reflecting stable velocity control. In contrast, stroke patients show greater velocity fluctuations. Especially when the velocity approaches zero, there will be brief fluctuations. Several factors may cause this phenomenon: 1) Stroke patients may take more time in the stages of picking up and putting down objects, resulting in a lower rate of velocity change in these two stages; 2) Muscle damage may lead to unstable hand control, especially when performing fine

movements. The impaired neuromuscular coordination function makes it difficult to maintain the smoothness of movement.

5.3 Convergent Validity Analysis

The effectiveness of the Nine Hole Peg Test (NHPT) has been relatively well confirmed in multiple studies. For example, scholars such as Lamers [33] conducted a motion study using the NHPT and the Action Research Arm Test (ARAT). The results showed that the NHPT could serve as a predictive indicator of hand movement performance, but the study did not mention the analysis of fine hand movements. Scholars such as Kuchtaruk [34] regarded the NHPT as the gold standard and compared it with the results of evaluating finger flexibility using the DIGITS joint tracking network application. Scholars such as Adiguzel [35] used the NHPT as one of the important indicators for evaluating the manual ability of patients with multiple sclerosis. By comparing the changes in NHPT scores before and after treatment, they judged the impact of neurodynamic mobilization on the hand flexibility of patients.

In addition, the Pearson correlation coefficient was used to explore further the association between all features and the total time, that is, the convergent validity of the features. The research results (as shown in [Table 7](#)) indicate that t_3 ($r=0.909$, $p<0.001$), t_4 ($r=0.855$, $p<0.001$), and the GRR ($r=0.907$, $p<0.001$) all show strong correlations. Among them, the r -score values of t_3 and t_4 match their excellent reliability performance in the ICC. In addition, V_{mean} and J^* show negative correlations in the Pearson correlation analysis (with r -scores of -0.765 and -0.833 , respectively, $p<0.001$), which reflects a significant negative relationship between these features and the total time. This is consistent with their good to excellent reliability ratings in the ICC, emphasizing their importance as metrics reflecting the efficiency and smoothness of hand movements. However, $V_{1\text{max}}$ ($r=0.282$, $p=0.309$) and $V_{2\text{max}}$ ($r=0.135$, $p=0.631$) have low r -score values in the Pearson correlation analysis, indicating that the relationships between these features and the total time may be weak. In conclusion, these data reveal a significant association between the time of specific movement stages, the hand movement function, the overall movement efficiency, and the total task execution time of stroke patients. The research of scholars such as Johansson [6] obtained a moderate to strong correlation between kinematic features and the NHPT score, especially the smoothness of the motion trajectory in the Return Stage, which is generally the same as the conclusion of this study. However, their research only involved healthy subjects and did not study the hand movements of stroke patients, limiting the applicability of the conclusion.

5.4 Clinical Potential Applications

Scholars such as Fischer [36] proposed a motion analysis plan to evaluate the movement of hand and finger joints by measuring the Range of Motion (ROM) of the subjects. The results show that this method has high repeatability and prove that ROM can be used as an effective evaluation metric. However, the study did not use fine motor movements as test actions, and the conclusion may have high limitations. In contrast, this study is based on the analysis of multiple metrics of fine motor movements, and the reliability of the conclusion is high. In conclusion, as shown in [Table 10](#), the hand feature dataset has been proven to be a reliable parameter for the quantitative evaluation of hand functionality based on the D-NHPT. These features not only demonstrate a correlation with clinical test scores but also effectively distinguish between stroke patients and healthy subjects, which is of great significance for detecting the differences in hand dexterity between healthy subjects and stroke patients.

Due to the high correlation shown by the Pearson correlation coefficient and the high reliability proven by the ICC, t_3 , t_4 , V_{mean} , and SAL can all serve as sensitive metrics for evaluating hand function, as shown in [Table 11](#). This is of great significance for the detailed analysis of the hand movements of stroke patients and the formulation of rehabilitation programs.

Based on the above analysis of various sensitive indicators of hand characteristics, these indicators have specific guiding significance in the assessment of hand function and rehabilitation training for stroke patients. Their clinical application pathways have been specified, and the closed-loop mechanism based on "indicator abnormality-functional impairment-intervention strategy" possesses the flexibility for dynamic adjustment. The rehabilitation team will adjust the training program in real time according to the patient's condition and indicator data: when the patient makes progress, the difficulty and intensity will be increased; when difficulties are encountered, the causes will be analyzed to optimize the program. This ensures the precision and targeting of rehabilitation treatment, enhances the conversion value of rehabilitation effects, and provides a scientific and systematic solution for the comprehensive recovery of the patient's hand function. Details are as follows: 1) Prolonged t_3 directly reflects fine motor control disorders of the hand in stroke patients (such as unstable grasping and inaccurate peg alignment). Clinically, t_3 can be used as a core indicator, and targeted grip strength training can be designed prioritizing "insertion movements" [37], among others. 2) The stability of t_4 makes it suitable as a long-term monitoring indicator; if a patient's t_4 shortens by $\geq 15\%$ compared to the baseline, it may indicate improved coordination of return movements, and the rehabilitation program can maintain its current intensity. 3) V_{mean} can quantify overall motor flexibility; when a patient's V_{mean} increases to 0.10m/s (close to the

mean of the healthy group, 0.108m/s), it suggests that the speed requirements for their daily activities (such as dressing and eating) may be met, and the training goal can be adjusted to refined control. 4) Improvement in *SAL* indicates enhanced motor continuity; clinically, priority can be given to selecting training items requiring continuous movements, such as ball games and puzzles, to strengthen the fluency of neural control [38].

In terms of training requirements, clinicians first need to be familiar with basic operations of the hand movement data acquisition system, including parameter configuration (such as subject ID, collection serial number, and collection mode), as well as starting and stopping data collection. Additionally, clinicians need to understand the key indicators in the hand feature dataset (as shown in Table 10), such as mean velocity (V_{mean}) and spectral arc length (*SAL*). They should also interpret the quantitative results of patients' hand movement function based on the patient's hand feature data output by the system (in CSV format) to provide patients with personalized rehabilitation treatment plans.

In the aspect of integration with electronic health records (EHRs), the hand feature dataset constructed by D-NHPT can be connected to the hospital's existing EHR system via standardized data interfaces. This enables the associated storage of multidimensional indicators from each patient's test, including their past medical history, imaging findings, and data from other rehabilitation assessment scales (e.g., FIM scores, Brunnstrom stages). It provides clinicians with longitudinal quantitative trajectories of hand function rehabilitation progress [37]. Meanwhile, the standardized data format supports data sharing and joint analysis in multi-center studies, laying a foundation for big data research on hand function rehabilitation in stroke. In remote monitoring and tele-rehabilitation applications, the LMC2-based non-contact hand movement data acquisition system is adaptable to simple setups in home environments, allowing patients to complete tests at home following standardized procedures [38]. Collected movement data is transmitted to clinical terminals via encrypted networks, enabling clinicians to remotely view visualized results such as index finger movement trajectories and speed change curves. They can evaluate rehabilitation outcomes based on dynamic changes in hand feature indicators and adjust training plans in a timely manner. This model is particularly suitable for long-term follow-up of patients with chronic stroke and rehabilitation management in areas with scarce medical resources. It breaks time and space barriers, achieves seamless integration of clinical assessment and rehabilitation intervention, and thereby enhances the continuity and accessibility of rehabilitation treatment.

5.5 Limitations / Future Work

Despite the positive outcomes of the study, several limitations remain:

- 1) First, the accuracy of the hand-motion data collection system is susceptible to environmental factors. Although the latest LMC2 was used to capture hand-motion data, misjudgments or data loss can still occur during the capture of rapid or complex gestures (especially when the background lighting is complex or the contrast is low). In the future, a dynamic calibration model based on deep learning is planned to be designed at the algorithm level. By real-time analysis of environmental lighting and background complexity, the tracking parameters of the LMC2 will be adaptively adjusted to enhance the stability and robustness of hand-motion data in complex scenarios.
- 2) Secondly, the small sample size has limited the validation of the generalizability of the hand feature dataset. In the future, it will be necessary to expand the sample size and quantify the impact of the factors mentioned above on feature indicators through stratified analysis, so as to enhance the applicability of D-NHPT in diverse clinical scenarios. In addition, the impact of key clinical variables has not been systematically analyzed. Factors such as stroke severity (e.g., lesion size and location) and cognitive status (e.g., MoCA scores) may interact with the results of hand function assessments. Future studies will comprehensively collect relevant data from subjects and incorporate these variables into a unified statistical analysis framework. By constructing a multiple regression model, the interaction and independent impact weights between various factors and the characteristic indicators of hand function assessment will be quantified.

6. Conclusion

This study successfully developed a computer vision-driven D-NHPT for stroke patients' hand function evaluation. By improving the traditional NHPT, collecting data with the LMC2, and establishing a hand feature dataset, we achieved a more objective and comprehensive assessment. The experimental results show that the D-NHPT has good reliability and validity and can effectively distinguish between stroke patients and healthy subjects. Moreover, the identified sensitive metrics provide valuable references for rehabilitation treatment (ICC=0.818–0.946 for the patient group, ICC=0.785–0.904 for the healthy group, discriminant validity $p < 0.019$, $|r\text{-score}| = 0.671\text{--}0.909$). Overall, this study further improves the digitalization level of clinical assessment scales for hand function in stroke patients and is expected to promote the development of relevant rehabilitation medicine.

References

- [1] D. Cao *et al.*, “Efficacy and safety of manual acupuncture for the treatment of upper limb motor dysfunction after stroke: Protocol for a systematic review and meta-analysis,” Nov. 01, 2021, *Public Library of Science*.
- [2] X. Q. Shi, H. L. Heung, Z. Q. Tang, Z. Li, and K. Y. Tong, “Effects of a Soft Robotic Hand for Hand Rehabilitation in Chronic Stroke Survivors,” *Journal of Stroke and Cerebrovascular Diseases*, vol. 30, no. 7, Jul. 2021.
- [3] I. Lamers, S. Kelchtermans, I. Baert, and P. Feys, “Upper Limb Assessment in Multiple Sclerosis: A Systematic Review of Outcome Measures and their Psychometric Properties,” *Arch Phys Med Rehabil*, vol. 95, no. 6, pp. 1184–1200, 2014.
- [4] E. Ekstrand, J. Lexell, and C. Brogårdh, “Test–Retest Reliability and Convergent Validity of Three Manual Dexterity Measures in Persons With Chronic Stroke,” *PM&R*, vol. 8, no. 10, pp. 935–943, 2016.
- [5] E. L. Proud, K. J. Miller, B. Bilney, M. E. Morris, and J. L. McGinley, “Construct validity of the 9-Hole Peg Test and Purdue Pegboard Test in people with mild to moderately severe Parkinson’s disease,” *Physiotherapy (United Kingdom)*, vol. 107, pp. 202–208, Jun. 2020.
- [6] G. M. Johansson and C. K. Häger, “A modified standardized nine hole peg test for valid and reliable kinematic assessment of dexterity post-stroke,” *J Neuroeng Rehabil*, vol. 16, no. 1, Jan. 2019.
- [7] J. Ma, J. Zhang, Y. Yang, B. Yang, and C. Shan, “Motor Imagery Classification Based on Temporal-Spatial Domain Adaptation for Stroke Patients,” *Cognit Comput*, vol. 17, no. 3, Jun. 2025.
- [8] M. Sui *et al.*, “A soft-packaged and portable rehabilitation glove capable of closed-loop fine motor skills,” *Nat Mach Intell*, vol. 5, pp. 1–12, Jul. 2023.
- [9] W. Y. Huang, Y. C. Du, and R. J. Cherng, “Feasibility study of kinect home-based aerobic exercise assessment for pre-frail community-dwelling older adults,” *J Med Biol Eng*, Jun. 2025.
- [10] Q. Xie, B. Sheng, J. Huang, Q. Zhang, and Y. Zhang, “A Pilot Study of Compensatory Strategies for Reach-to-Grasp-Pen in Patients with Stroke,” *Appl Bionics Biomech*, vol. 2022, 2022.

- [11] B. Sheng, X. Lei, J. Cheng, Q. Xie, J. Tao, and Y. Chen, "Novel Digital Assessment System for Upper-Limb Movement in Stroke Patients Using Markless-Sensing Technology and Deep Learning Algorithms," *J Shanghai Jiaotong Univ Sci*, 2024.
- [12] B. Sheng, J. Zhao, J. Zheng, C. Duan, S. Q. Xie, and J. Tao, "A Study of Hand Function in Stroke Patients Using Kinematic Metrics," *IEEE/ASME International Conference on Advanced Intelligent Mechatronics, AIM*, vol. 2023-June, pp. 777–782, 2023.
- [13] P. Feys *et al.*, "The Nine-Hole Peg Test as a manual dexterity performance measure for multiple sclerosis," Apr. 01, 2017, *SAGE Publications Ltd*.
- [14] F. Temporiti *et al.*, "Kinematic evaluation and reliability assessment of the Nine Hole Peg Test for manual dexterity," *Journal of Hand Therapy*, vol. 36, no. 3, pp. 560–567, 2023.
- [15] M. Gil-Martín, M. R. Marini, R. San-Segundo, and L. Cinque, "Dual Leap Motion Controller 2: A Robust Dataset for Multi-view Hand Pose Recognition," *Sci Data*, vol. 11, no. 1, p. 1102, Dec. 2024.
- [16] B. Chakravarthi, P. P. B. M, and P. K. B. N, "A Comprehensive Review of Leap Motion Controller-based Hand Gesture Datasets," Nov. 2023.
- [17] Y. Bai and D. Wang, "On the comparison of trilinear, cubic spline, and fuzzy interpolation methods in the high-accuracy measurements," *IEEE Transactions on Fuzzy Systems*, vol. 18, no. 5, pp. 1016–1022, Oct. 2010.
- [18] H. Hassani, "Singular Spectrum Analysis: Methodology and Comparison," *Journal of Data Science*, vol. 5, no. 2, pp. 239–257, Jul. 2021.
- [19] F. J. Alonso, J. M. D. Castillo, and P. Pintado, "Application of singular spectrum analysis to the smoothing of raw kinematic signals," *J Biomech*, vol. 38, no. 5, pp. 1085–1092, 2005.
- [20] A. Ozturk, A. Tartar, B. Ersoz Huseyinsinoglu, and A. H. Ertas, "A clinically feasible kinematic assessment method of upper extremity motor function impairment after stroke," *Measurement*, vol. 80, pp. 207–216, 2016.
- [21] A. Khan, M. Atikur, R. Khan, D. S. Poskitt, and D. S. Poskitt, "Window Length Selection and Signal-Noise Separation and Reconstruction in Singular Spectrum Analysis Window Length Selection and Signal-Noise Separation and Reconstruction in Singular Spectrum Analysis Window Length Selection and Signal-Noise Separation and Reconstruction in Singular Spectrum Analysis," 2011.
- [22] S. M. Shaharudin, N. Ahmad, and F. Yusof, "Effect of window length with singular spectrum analysis in extracting the trend signal on rainfall data," in *AIP Conference Proceedings*, American Institute of Physics Inc., 2015, pp. 321–326.
- [23] I. Carpinella, J. Jonsdottir, and M. Ferrarin, "Multi-finger coordination in healthy subjects and stroke patients: a mathematical modelling approach," *J Neuroeng Rehabil*, vol. 8, pp. 19–19, 2011.

- [24] B. Rohrer *et al.*, "Movement Smoothness Changes during Stroke Recovery," 2002.
- [25] S. Balasubramanian, A. Melendez-Calderon, and E. Burdet, "A robust and sensitive metric for quantifying movement smoothness," *IEEE Trans Biomed Eng*, vol. 59, no. 8, pp. 2126–2136, 2012.
- [26] S. Balasubramanian, A. Melendez-Calderon, A. Roby-Brami, and E. Burdet, "JNER JOURNAL OF NEUROENGINEERING AND REHABILITATION On the analysis of movement smoothness," *J Neuroeng Rehabil*, vol. 12, p. 112, 2015.
- [27] B. Sheng *et al.*, "A novel scoring approach for the Wolf Motor Function Test in stroke survivors using motion-sensing technology and machine learning: A preliminary study," *Comput Methods Programs Biomed*, vol. 243, no. December 2022, p. 107887, 2024.
- [28] N. Hogan and D. Sternad, "Sensitivity of smoothness measures to movement duration, amplitude, and arrests," *J Mot Behav*, vol. 41, no. 6, pp. 529–534, 2009.
- [29] L. Meng *et al.*, "Automatic Upper-Limb Brunnstrom Recovery Stage Evaluation via Daily Activity Monitoring," *IEEE Transactions on Neural Systems and Rehabilitation Engineering*, vol. 30, pp. 2589–2599, 2022.
- [30] K. Miyata, S. Tamura, S. Kobayashi, R. Takeda, and H. Iwamoto, "BERG BALANCE SCALE IS A VALID MEASURE FOR PLAN INTERVENTIONS AND FOR ASSESSING CHANGES IN POSTURAL BALANCE IN PATIENTS WITH STROKE," *J Rehabil Med*, vol. 54, 2022.
- [31] T. K. Koo and M. Y. Li, "A Guideline of Selecting and Reporting Intraclass Correlation Coefficients for Reliability Research," *J Chiropr Med*, vol. 15, no. 2, pp. 155–163, Jun. 2016.
- [32] H. Akoglu, "User's guide to correlation coefficients," Sep. 01, 2018, *Emergency Medicine Association of Turkey*.
- [33] I. Lamers, L. Kerkhofs, J. Raats, D. Kos, B. Van Wijmeersch, and P. Feys, "Perceived and actual arm performance in multiple sclerosis: relationship with clinical tests according to hand dominance," *Multiple Sclerosis Journal*, vol. 19, pp. 1341–1348, Feb. 2013.
- [34] A. Kuchtaruk *et al.*, "Assessment of finger dexterity through the DIGITS joint tracking web application—An evaluation study with comparison to the nine-hole pegboard test," *Journal of Hand Therapy*, vol. 37, no. 3, pp. 438–445, 2024.
- [35] H. Adiguzel Tat, Z. I. K. Kirmaci, S. Erel, Y. Inanç, and D. T. Berktaş, "The effects of Neurodynamic Mobilization exercises on upper extremity pain, muscle strength, and functions in patients with multiple sclerosis: A randomised controlled, single blinded study," *Mult Scler Relat Disord*, vol. 93, p. 106240, 2025.
- [36] G. Fischer, D. Jermann, R. List, L. Reissner, and M. Calcagni, "Development and application of a motion analysis protocol for the kinematic evaluation of basic and functional hand and finger movements using motion capture in a clinical setting-A repeatability study," *Applied Sciences (Switzerland)*, vol. 10, no. 18, Sep. 2020.

- [37] C. Bausewein *et al.*, “Implementing patient reported outcome measures (PROMs) in palliative care - users’ cry for help,” *Health Qual Life Outcomes*, vol. 9, Apr. 2011.
- [38] S. He, S. Huang, L. Huang, F. Xie, and L. Xie, “LiDAR-Based Hand Contralateral Controlled Functional Electrical Stimulation System,” *IEEE Transactions on Neural Systems and Rehabilitation Engineering*, vol. 31, pp. 1776–1785, 2023.

Declarations of interest

The authors declare that they have no known competing financial interests or personal relationships that could have appeared to influence the work reported in this paper.

Funding

This work was supported by the International Exchanges 2023 Cost Share (NSFC-Royal Society) under Grants [IES\R3\233204](#), the National Natural Science Foundation of China under Grants [62103252](#) and [82305357](#), and the Shanghai Magnolia Talent Plan Pujiang Project under Grants [24PJA032](#).

Consent to participate

Informed consent was obtained from all individual participants included in the study.

Consent to publish

The authors affirm that human research participants provided informed consent for publication of the images in Figures 7, 8, and 9, and the data in Tables 2, 4, 5, 6, 7 and 8.

Ethical approval

The ethical approval has been given by the Ethics Committee of Shanghai University (Approval No.: ECSHU 2021-102). Informed consent was obtained from all participants.

Data Availability Statement

The data that support the findings of this study are available from the corresponding author, [Bo Sheng], upon reasonable request.

CRedit authorship contribution statement

Yuxin Fan: Conceptualization, Methodology, Software, Writing – original draft. **Aiqin Liu**: Formal analysis. **Qiurong Xie**: Writing – review& editing, Supervision. **Qi Zhang**:

Writing – review & editing. **Jianyu Zhao**: Writing – review & editing. **Sheng Quan Xie**: Investigation, Writing – review & editing. **Bo Sheng**: Validation, Supervision

Appendix

Table 1 Definitions and Transition Criteria for Hand Movement Stages of D-NHPT

Stage Name	Definition	Transition Criteria
Picking-up Stage	The patient touches the peg with the thumb and index finger until the peg is completely removed from the hole	Between the end of the previous Returning Stage and the start of the current Moving Stage
Moving Stage	The patient moves the peg from the removed position to above the next predetermined insertion hole	The Moving Stage is considered to start when the speed of the tip of the index finger exceeds 5% of the maximum speed and lasts for at least 40 ms; it is considered to end when the speed of the tip of the index finger drops below 5% of the maximum speed and lasts for at least 40 ms
Placing Stage	The patient inserts the peg into the hole, and the fingers completely leave the peg	Between the end of the previous Moving Stage and the start of the current Returning Stage
Returning Stage	The patient's hand moves to the next peg and prepares for the next pick-up action	The Returning Stage is considered to start when the speed of the tip of the index finger exceeds 5% of the maximum speed and lasts for at least 40 ms; it is considered to end when the speed of the tip of the index finger drops below 5% of the maximum speed and lasts for at least 40 ms

Table 2 The detailed information on the extracted features

Type	Name	Clinical Significance	Ref
Time	<i>Total Time, T</i>	Hand movement efficiency	[6,14]
	<i>Time of the Picking-up Stage, t₁</i>	Hand flexibility	[6,14]
	<i>Time of the Moving Stage, t₂</i>	Hand motor function	[6,14]
	<i>Time of the Placing Stage, t₃</i>	Hand flexibility	[6,14]
	<i>Time of the Returning Stage, t₄</i>	Hand motor function	[6,14]
<u>Kinematics</u>	<i>Grasp-Reach Ratio, GRR</i>	Hand coordination	[6]
	<i>Angle Range</i>	Hand flexibility	[23]

<i>Index Finger Path Ratio, Path</i>	Hand movement efficiency	[6]
<i>Peak Velocity at the Moving Stage, V_{1max}</i>		N/A
<i>Peak Velocity at the Returning Stage, V_{2max}</i>	Hand motor function	N/A
<i>Average Velocity, V_{mean}</i>		N/A
<i>Spectrum Arc Length, SAL</i>	Smoothness of hand	[26]
<i>Dimensionless Jerk, J^*</i>	movement	[28]

Table 3 Basic Information Table of Subjects

Subject ID	Gender	Age	Phases of Stroke	Affected Hand	Dominant Hand	Brunnstrom Stage	Berg Balance Score
P1	Male	45	90	Right Hand	Right Hand	VI	53
P2	Male	81	65	Left Hand	Right Hand	VI	24
P3	Female	46	25	Left Hand	Right Hand	VI	50
P4	Male	40	49	Left Hand	Right Hand	V	50
P5	Male	59	73	Right Hand	Right Hand	V	26
P6	Male	61	43	Left Hand	Right Hand	V	9
P7	Male	70	41	Left Hand	Right Hand	VI	52
P8	Male	56	57	Right Hand	Right Hand	VI	42
P9	Male	45	28	Left Hand	Right Hand	V	49
P10	Male	67	22	Left Hand	Right Hand	VI	52
H1	Male	24	N/A	N/A	Right Hand	N/A	N/A
H2	Male	24	N/A	N/A	Right Hand	N/A	N/A
H3	Male	25	N/A	N/A	Right Hand	N/A	N/A
H4	Female	23	N/A	N/A	Right Hand	N/A	N/A
H5	Female	24	N/A	N/A	Right Hand	N/A	N/A

Table 4 Brunnstrom 6 Stages of Motor Recovery

Stage	Characteristics
Stage I	The affected limb is completely flaccid with no voluntary movement or reflexes.
Stage II	Spasticity begins to develop, and basic limb synergies or primitive movement patterns may emerge.
Stage III	Spasticity peaks, and voluntary movement is limited to basic synergies (flexor or extensor patterns).
Stage IV	Spasticity decreases, and some movement patterns outside of synergies become possible.
Stage V	Spasticity further decreases, and more complex movement combinations are achieved.
Stage VI	Spasticity is minimal or absent, and near-normal motor control is restored.

Table 5 ICC and 95% CI of Features for All Participants in the Digitalized Nine Hole Peg Test

Feature	Stroke Patients			Healthy Subjects		
	ICC	CI 95%	p-value	ICC	CI 95%	p-value
T	0.858	[0.770,0.913]	<0.001	0.890	[0.848,0.921]	<0.001
t_1	0.939	[0.516,0.944]	<0.001	0.811	[0.761,0.901]	<0.001
t_2	0.824	[0.612,0.926]	<0.001	0.764	[0.665,0.806]	<0.001
t_3	0.921	[0.821,0.965]	<0.001	0.904	[0.855,0.936]	<0.001
t_4	0.946	[0.830,0.984]	<0.001	0.785	[0.719,0.838]	<0.001

<i>GRR</i>	0.703	[0.676,0.876]	<0.001	0.714	[0.626,0.759]	<0.001
<i>Path</i>	0.729	[0.671,0.805]	<0.001	0.795	[0.764,0.823]	<0.001
<i>Angle Range</i>	0.539	[0.486,0.551]	<0.001	0.849	[0.794,0.886]	<0.001
V_{1max}, V_{2max}	0.631	[0.512,0.724]	<0.001	0.749	[0.738,0.801]	<0.001
V_{mean}	0.818	[0.789,0.873]	<0.001	0.826	[0.781,0.865]	<0.001
<i>SAL</i>	0.922	[0.906,0.967]	<0.001	0.892	[0.883,0.925]	<0.001
J^*	0.610	[0.552,0.741]	<0.001	0.724	[0.578,0.814]	<0.001

Table 6 Time Features for All Participants in the Digitalized Nine Hole Peg Test

Subject ID	<i>T</i>(s)	t_1(s)	t_2(s)	t_3(s)	t_4(s)	<i>GGR</i>
P1	50.19	18.36	7.02	22.51	4.95	3.18
P2	53.22	19.92	9.79	18.5	7.23	2.26
P3	65.53	15.16	9.22	33.78	6.25	3.16
P4	40.21	10.14	8.79	14.5	7.11	1.55
P5	100.92	11.67	7.22	90.99	7.64	6.91
P6	23.36	6.16	5.52	7.81	3.89	1.49
P7	22.4	4.71	3.83	10.64	3.22	2.17
P8	50.13	19.45	5.01	19.92	5.21	3.85
P9	57.20	22.29	12.54	19.43	8.09	2.02
P10	20.7	4.96	4.28	8.12	3.36	1.71
H1	12.75	2.28	3.18	4.27	3.02	1.05
H2	13.8	2.54	3.89	3.76	3.61	0.84
H3	13.5	1.97	4.14	3.67	3.72	0.71
H4	11.65	1.86	3.36	3.58	2.85	0.87
H5	12.6	1.7	3.75	3.36	2.95	0.76

Table 7 Kinematic Features for All Participants in the Digitized Nine Hole Peg Test

Subject ID	<i>T</i>	<i>Path</i>	<i>Angle Range</i>	V_{1max}	V_{2max}	V_{mean}	<i>SAL</i>	J^*
P1	50.19	1.21	10.94	0.53	0.62	0.07	-35.45	-31.53
P2	53.22	1.25	14.85	0.28	0.31	0.07	-35.22	-27.11
P3	65.53	1.46	19.83	0.93	1.16	0.07	-34.27	-32.86
P4	40.21	1.23	11.33	0.19	0.25	0.06	-42.27	-28.54
P5	100.92	1.93	12.6	0.28	0.21	0.06	-46.82	-39.7
P6	23.36	1.62	9.55	0.36	0.43	0.12	-49.3	-33.37
P7	22.4	1.00	8.30	0.29	0.34	0.11	-5.1	-28.53
P8	50.13	1.53	10.3	0.31	0.26	0.08	-11.34	-31.61
P9	57.20	1.23	10.8	0.2	0.26	0.05	-19.84	-31.09
P10	20.7	1.06	9.04	0.4	0.68	0.11	-6.44	-27.57
H1	12.75	1.15	39.83	0.25	0.33	0.10	-5.8	-26.6

H2	13.8	1.10	35.08	0.26	0.30	0.11	-5.2	-27.11
H3	13.5	1.05	35.32	0.32	0.39	0.14	-5.57	-27.03
H4	11.65	1.14	35.55	0.27	0.29	0.09	-8.13	-26.29
H5	12.6	1.28	29.52	0.25	0.26	0.10	-6.86	-26.53

Note: The unit of *Angle Range* is degrees (°); the units of $V_{1\max}$, $V_{2\max}$, and V_{mean} are all m/s.

Table 8 Pearson Correlation Coefficients between All Hand Features and Total Time

Feature	r-score	p-value
t_1	0.74	0.002
t_2	0.693	0.004
t_3	0.909	<0.001
t_4	0.855	<0.001
GRR	0.907	<0.001
<i>Path</i>	0.724	0.002
<i>Angle Range</i>	-0.543	<0.001
$V_{1\max}$	0.282	0.309
$V_{2\max}$	0.135	0.631
V_{mean}	-0.765	<0.001
SAL	-0.671	0.006
J^*	-0.833	<0.001

Table 9 Mean Difference and Standard Error of Hand Features

Feature	Mean Value of Patient Group	Mean Value of Healthy Group	MD	SE	p-value
T	48.386s	12.86s	35.526s	7.65s	<0.001
t_1	13.282s	2.07s	11.212s	2.20s	<0.001
t_2	7.322s	3.664s	3.658s	0.95s	0.002
t_3	24.62s	3.73s	20.89s	8.04s	0.019
t_4	5.695s	3.23s	2.465s	0.57s	<0.001
GRR	2.83	0.846	1.984	0.52	0.001
<i>Angle Range</i>	11.754°	35.06°	-23.306°	1.96°	<0.001
<i>Path</i>	1.352mm	1.144mm	0.208mm	0.10mm	0.036
$V_{1\max}$	0.377m/s	0.270m/s	0.087m/s	0.071m/s	0.231
$V_{2\max}$	0.452m/s	0.314m/s	0.138m/s	0.096m/s	0.166
V_{mean}	0.08m/s	0.108m/s	-0.028m/s	0.01m/s	0.014
SAL	-28.605	-6.312	-22.293	4.80	<0.001
J^*	-31.191	-26.712	-4.479	1.32	0.003

Table 10 Hand Feature Dataset

Type	Feature
Sensitive Metrics	t_3
	t_4
	V_{mean}
	SAL
	GGR
Exploratory Metrics	Angle Range
	Path
	J^*
	t_1
	t_2

Table 11 Hand Sensitive Metrics

Feature	Within-group Reliability		Discriminant Validity	Convergent Validity
	Patient Group	Healthy Group	p -value	r -score
e	ICC	ICC		
t_3	0.921	0.904	0.019	0.909
t_4	0.946	0.785	<0.001	0.855
V_{mean}	0.818	0.826	0.014	-0.765
SAL	0.922	0.892	<0.001	-0.671